KERNFORSCHUNGSZENTRUM

KARLSRUHE

März 1974 KFK 1943

Institut für Experimentelle Kernphysik

Beta Decay and Nuclear Structure: Rb^{86}

H. Appel, H. Behrens, K. Bürk,
H.-W. Müller, L. Szybisz, R. Wischhusen

GESELLSCHAFT
FÜR
KERNFORSCHUNG M.B.H.

KARLSRUHE

GESELLSCHAFT FÜR KERNFORSCHUNG M.B.H.
KARLSRUHE

KERNFORSCHUNGSZENTRUM KARLSRUHE

KFK 1943

Institut für Experimentelle Kernphysik

Beta Decay and Nuclear Structure: Rb^{86}

H. Appel, H. Behrens, K. Bürk, H.-W. Müller, L. Szybisz
and R. Wischhusen

Gesellschaft für Kernforschung m.b.H., Karlsruhe

Abstract:

It was aimed to gain information on the nuclear structure of Rb^{86} by investigation of the $2^- \rightarrow 2^+$ β transition. For this purpose the energy dependence of the $\beta\gamma$ angular correlation and the angle dependence of the $\beta\gamma$ circular polarization correlation have been measured. A novel experimental set-up has been used for the angular correlation measurement allowing a simultaneous determination of the anisotropy coefficients A_2 and A_4 under considerable reduction of systematical and statistical errors. For the polarization correlation measurement an unusual experimental arrangement has been applied providing the possibility of simultaneous observation under four different angles. Employing additional data on shape factor measurements and energy dependent circular polarization correlations from other authors the nuclear structure of the 2^- state in Rb^{86} and the 2^+ first excited state in Sr^{86} have been evaluated. For the latter purpose the unified model with weak coupling has been chosen.

Das Ziel der vorliegenden Arbeit ist es, Information über die Kernstruktur von Rb^{86} durch die Untersuchung des $2^- \rightarrow 2^+$ β Übergangs zu erhalten. Dafür wurde die Energieabhängigkeit der $\beta\gamma$ Winkelkorrelation und die Winkelabhängigkeit der $\beta\gamma$ Zirkularpolarisationskorrelation gemessen. Für die Winkelkorrelationsmessung wurde eine neue experimentelle Anordnung benutzt, die die simultane Bestimmung der Anisotropiekoeffizienten A_2 und A_4 bei wesentlicher Verringerung der systematischen und statistischen Fehler erlaubt. Für die Polarisationskorrelationsmessung wurde eine neuartige Experimentieranordnung verwandt, die die simultane Beobachtung unter vier verschiedenen Winkeln ermöglicht. Unter Benutzung zusätzlicher Daten von Shape-Faktor-Messungen und energieabhängigen Zirkularpolarisationskorrelationen von anderen Autoren wurde die Kernstruktur des 2^--Zustandes in Rb^{86} und des ersten angeregten 2^+-Zustandes in Sr^{86} berechnet. Für die Rechnungen wurde das unified model mit schwacher Kopplung gewählt.

I. Introduction

With 49 neutrons Rb^{86} presents a nearly semi magic shell model configuration. Employing the simple shell model, one expects

for neutrons $(1g_{9/2})^{-1}$ and

for protons $(1f_{5/2})^{-1}$

coupled to 2^- for the ground state of Rb^{86}. The wave function being

$$|Rb^{86};\ 2^-> = |(1g_{9/2})^{-1}_{J=9/2\ v=1}\ (1f_{5/2})^{-1}_{J=5/2\ v=1};\ 2^-> \qquad (1)$$

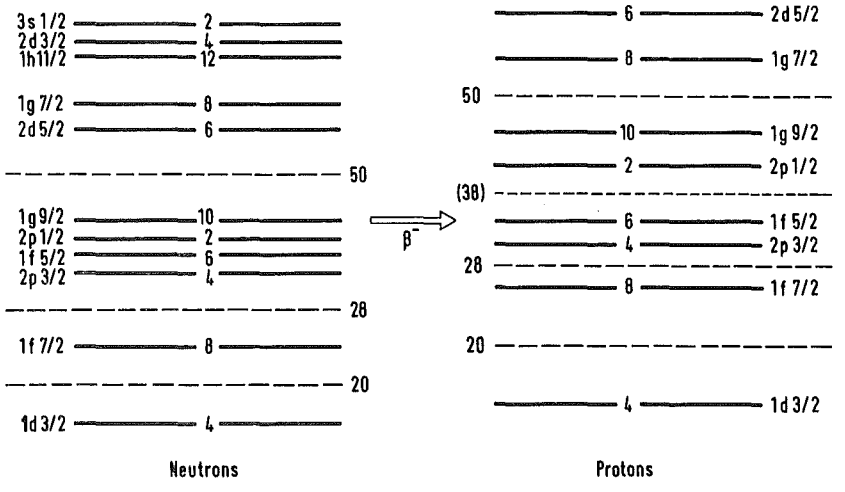

Fig.1. Schematic representation of the shell model levels around 49 neutrons and 37 protons

As can be taken from fig.1 no other combination of two closed by states within the relevant major shells leads to a 2^- state.

Rb^{86} decays by a unique first forbidden β-decay to the 0^+ -ground state of Sr^{86} and by a non-unique first forbidden transition to the first excited 2^+- state of this nucleus:

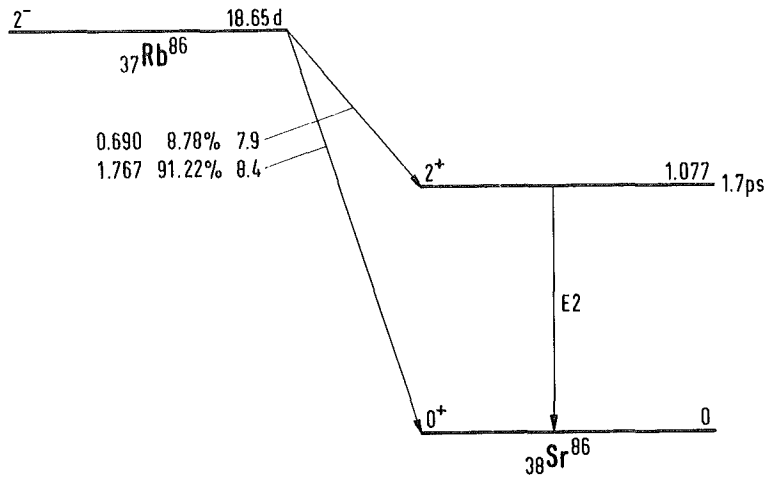

Fig.2. Decay scheme of Rb^{86}

In the simple shell model picture chosen, the ground state configuration for Sr^{86} would be for neutrons

$$|Sr^{86};\ 0^+> = |(1g_{9/2})^{-2}_{J=0,\ v=0};\ 0^+> \qquad (2)$$

This first excited state of Sr^{86} could then be interpreted with v = 2, namely as

$$|Sr^{86};\ 2^+> = |(1g_{9/2})^{-2}_{J=2,\ v=2};\ 2^+> \qquad (3)$$

Both β-decays should then be

$$\nu 1g_{9/2} \rightarrow \pi 1f_{5/2}$$

transitions. As a consequence only matrix elements of rank 2 or higher should contribute to the $2^- \rightarrow 2^+$ non unique transition as to the unique $2^- \rightarrow 0^+$ transition. All observable quantities for both transitions should, therefore, show the characteristic features of unique forbidden decays.

The experimental results for the $2^- \rightarrow 2^+\beta$ transition (i.e. the $\beta\gamma$ angular correlation, $\beta\gamma$ circular polarization correlation and shape factor measurements) do not support this simple shell model interpretation. Disregarding the microscopic picture and refering to initial and final states of the transition only, also matrix elements of rank 0 and 1 could contribute. Since the dominant matrix element in the shell model picture, i.e. the matrix element of rank 2 is reduced by factors pR or qR*, any admixture of matrix elements of rank 0 or 1 is relatively enhanced by this factor. Thus the observables from this decay are rather sensitive to configuration mixing that leads to such matrix elements of rank 0 and 1.

Both β transitions of Rb^{86} have been thoroughly treated theoretically, e.g. by Wahlborn |1|. The relatively easy experimental access to this nucleus has led to numerous investigations as regards to the shape factor |2-7|, the $\beta\gamma$ angular correlation |3,8-15|, the $\beta\gamma$ circular polarization correlation |6,7,11,16-19|, and also nuclear reactions of the types (p,t) and (d,t) |20,21|. In addition the magnetic dipole |22| and electric quadruopole moment have been determined |23|.
The investigations reported below aimed accurate results which might be interpreted in terms of nuclear structure. Some of the precedingly cited papers are contradictious or are lacking sufficient accuracy. In addition these papers usually extract single matrix elements from the observables |19,24-26|. The results on the $\beta\gamma$ angular correlation and the $\beta\gamma$ circular polarization correlation presented in the following chapters have been directly used to gain information on the nuclear structure of the nucleus Rb^{86}.

---

* where p and q are electron and neutrino momentum, respectively, and R being the nuclear radius.

II. The Experiment

In this chapter we shall describe the two experimental apparatus used for the measurements: arrangements to determine the βγ angular correlation and the βγ circular polarization correlation. For both set-ups emphasis has been laid on the use of high efficiency multi-detector arrangements which allow sufficiently good statistics and provide possibilities to eliminate instrumental and geometrical asymmetries.

II. 1. The βγ angular correlation measurement

An experimental set-up has been developed employing 4 β- and 2 periodically exchangeable γ-counters. Details are shown in fig. 3.

It is necessary to interchange the two γ-counters with respect to their positions in order to eliminate the βγ coincidence efficiencies. The main advantages of this arrangement are

- to register 8 βγ coincidence rates at the same time
- to measure the quantities A_2 and A_4 simultaneously
- the possibility to reduce systematic errors by a suitable data reduction technique and
- no correction for the source strength is necessary.

The chamber with the 4 β- counters can be turned by 45° to both sides of the symmetric position. The measurements under these different angle positions allow the determination of

- the unwanted γγ-coincidence counting rates resulting from counter to counter scattering
- the influence of bremsstrahlung effects originating from source or β-detectors
- the order of magnitude of the effects from β-back-

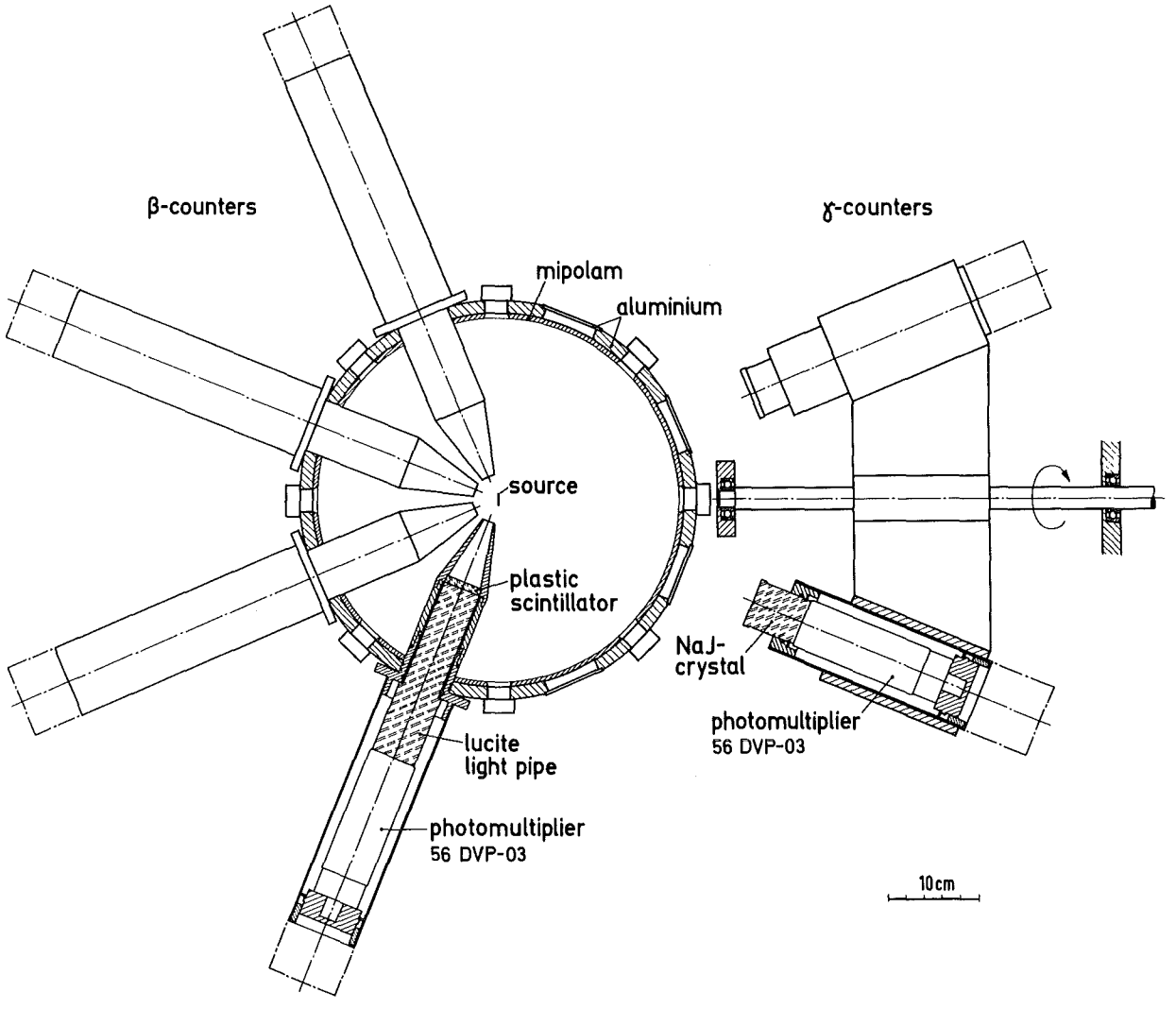

Fig.3. Experimental set-up for measuring βγ angular correlations

scattering and β-multiscattering within the source.

In fig.4. a schematic diagram of the possible positions of the β- and γ-counters is given.

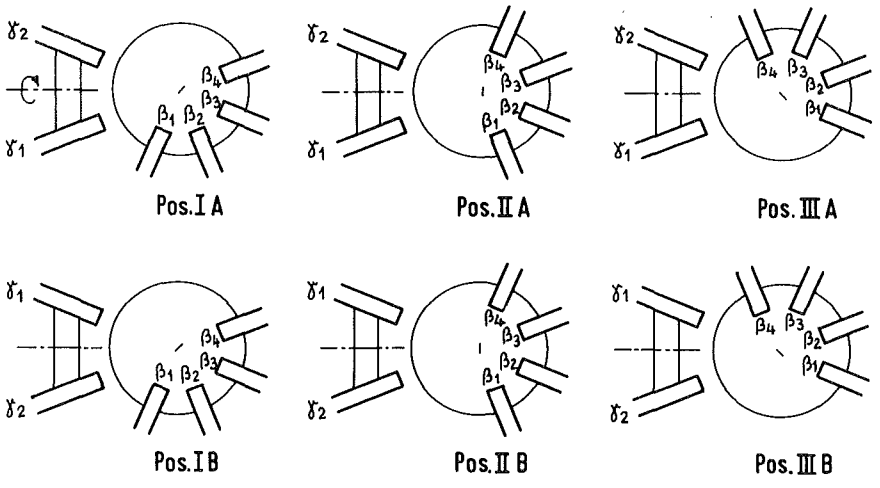

Fig.4. Schematic diagram of possible positions of the β- and γ-counters during the measurement of βγ-angular correlations

The anisotropy coefficients A_2 and A_4 of the angular correlation (for the definition see refs. |30-32|) have been evaluated in terms of quantities Q as follows:

$$A_2 = \frac{10}{7} \cdot \frac{4 - 9\sqrt[4]{\frac{Q_{m,A}}{Q_{m,B}}} + 5\sqrt[4]{\frac{Q_{n,A}}{Q_{n,B}}}}{8 + 6\sqrt[4]{\frac{Q_{m,A}}{Q_{m,B}}} + \sqrt[4]{\frac{Q_{n,A}}{Q_{n,B}}}} \qquad (4a)$$

$$A_4 = \frac{48}{7} \cdot \frac{-2 + \sqrt[4]{\frac{Q_{m,A}}{Q_{m,B}}} + \sqrt[4]{\frac{Q_{n,A}}{Q_{n,B}}}}{8 + 6\sqrt[4]{\frac{Q_{m,A}}{Q_{m,B}}} + \sqrt[4]{\frac{Q_{n,A}}{Q_{n,B}}}} \qquad (4b)$$

The positions of the β-detectors are represented by the Roman numbers (see fig.4.). The first indices for the Q's in equation (4) are

in position I : m = 1, n = 2
II : m = 3, n = 4
III : m = 2, n = 1

The second index for the Q's, i.e. A or B, respectively, denotes the two possible positions of the γ-counters. The quantities Q are:

$$Q_1 = \frac{K_{12} \cdot K_{21}}{K_{11} \cdot K_{22}}; \qquad Q_2 = \frac{K_{32} \cdot K_{41}}{K_{31} \cdot K_{42}}; \qquad Q_3 = \frac{K_{11} \cdot K_{42}}{K_{12} \cdot K_{41}}$$

$$Q_4 = \frac{K_{22} \cdot K_{31}}{K_{21} \cdot K_{32}} \qquad (5)$$

where K_{ij} is the true coincidence rate between the β-counter i and the γ-counter j.
The experimental data have been taken onto tape and evaluated according to the precedingly presented scheme. Characteristic for the electronic outlay was the use of fast-slow circuits in the γ-branch in order to discriminate the photo peak and the application of only fast differential discriminators for the β-branch.

Data output, change of counter positions (typical periods 300 sec) and determination of random coincidences have been mastered automatically.

Effects of bremsstrahlung and multiple- or backscattering of electrons within the source result in different values for the anisotropy coefficients in position II and I (or III), respectively.*
While from the point of view of the anisotropy coefficients the angles 45 and 135 degrees are equivalent, this is not true any more for electron bremsstrahlung coincidences. This problem has been encountered as follows: The use of a energetically suitable β-emitter (not accompanied by a succeeding γ-transition) allows a seperate determination of the angular correlation of these false coincidences. Their fractional contribution in the real experiment can be evaluated by forming the ratio

$$T = \left(\frac{\sqrt[4]{\frac{Q_{4,A}}{Q_{4,B}}}}{\sqrt[4]{\frac{Q_{3,A}}{Q_{3,B}}}} \right)_{I} \cdot \left(\frac{\sqrt[4]{\frac{Q_{4,A}}{Q_{4,B}}}}{\sqrt[4]{\frac{Q_{3,A}}{Q_{3,B}}}} \right)_{III} \sim \frac{\omega(135^{\circ})}{\omega(45^{\circ})} \qquad (6)$$

T should be equal to 1 in the absence of any coincidences not due to the investigated β-γ-cascade.

In the vicinity of the observed γ-energy (1.078 MeV) the bremsstrahlung intensity originating from the 1.78 MeV β-transition is still low. Thus the electron bremsstrahlung coincidence counting rate turned out to be very small, i.e. T deviated from the value 1 only within the statistical error.

---

* Bremsstrahlung preferably produced in the β-crystals leads to false coincidences by detection of the electron in a β-detector and the bremsstrahlung quantum in one of the γ-detectors. Thus, the false coincidence rate is enhanced in positions I or III (see fig.4.) for close by β- and γ-detectors.

The problem of multiple scattering of electrons in the source and its backing deserves a careful consideration. Usually the details are treated according to the formalism developed by Goudsmit and Saunderson |33| and Frankel |34| which is particulary suitable for corrections that have to be applied to angular correlation measurements as has been demonstrated experimentally, for example, by Gupta and Sastry |35|. This is not surprising since the formalism cited is developed in a series of Legendre polynomials as usual for angular correlations.

The evaluation coefficients are available analytically as long as Born approximation is applicable for the single scattering process and special assumptions for the screening by the electron shells are realistic. This method is, however, applicable only for geometries which are axial symmetric with respect to the direction source-detector. For the experimental arrangement, described here (see fig. 3), where angles of 22.5^{o} and 67.5^{o} appear with respect to the normal direction on the source, this formalism cannot be employed. A development in a series of spherical harmonics has to be used instead. Lacking the possibility to provide the evaluation coefficients analytically Monte Carlo methods seemed to be useful.

A special example for the influence of multiple electron scattering is plotted in fig. 5 for a β-energy of 200 and 500 keV as a function of the source thickness and the angle position. Details of the mathematical treatment are presented in appendix A |36|.

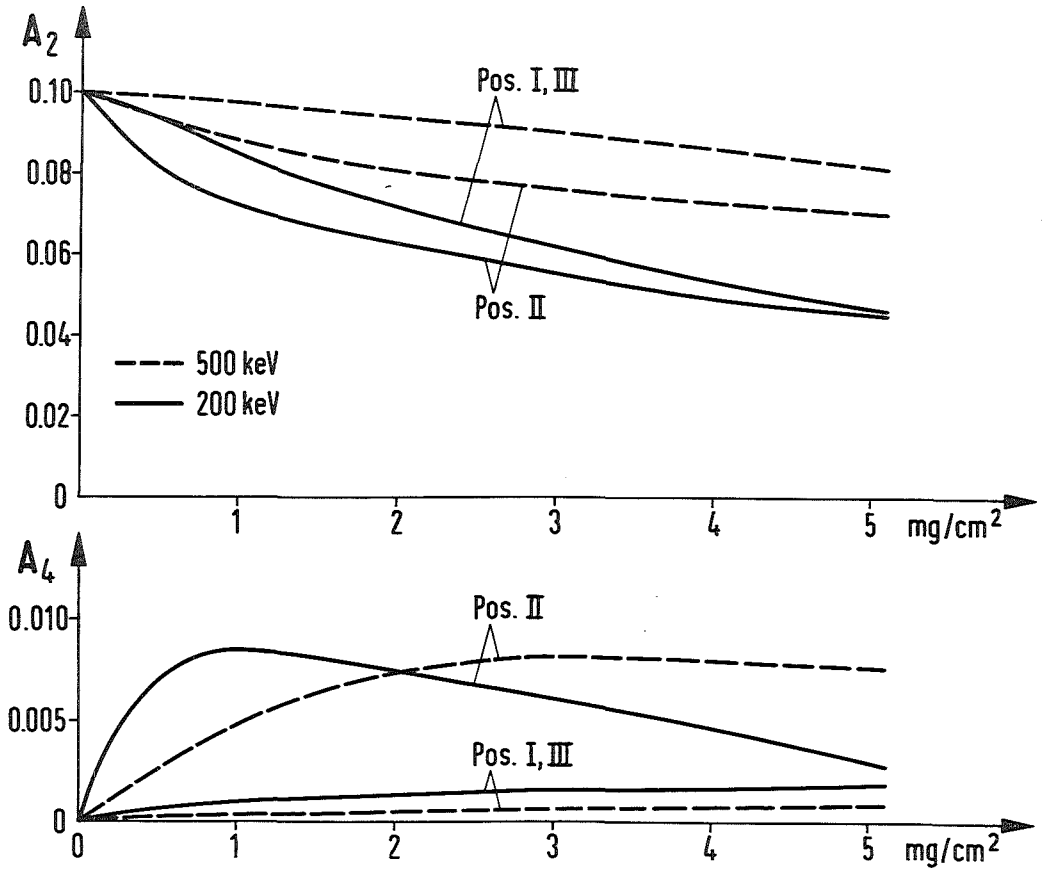

Fig.5. Influence of multiple electron scattering in the source on the asymmetry coefficients A_2 and A_4 as a function of the source thickness (mg/cm^2) for Rb^{86} for two representative β^- energies. The uncorrected anisotropy coefficients A_2 and A_4 have been chosen to 0.1 and 0, respectively. Note, that even for A_4=0 a finite value for A_4 may be observed, which is simulated by multiple scattering effects in the source only.

For multiple electron scattering processes in the source backing a similar procedure has been applied.

Finally, the finite solid angle for the detectors has been considered. For cylindrical detectors and a point source (this assumption is realistic in the presented case) the finite size of the detectors results in an attenuation of the correlation |34|

$$A_{k,corr} = a_k \cdot A_k = a_k^{\beta} \cdot a_k^{\gamma} \cdot A_k \quad . \qquad (7)$$

The factors a_k have been calculated considering the reduced detection efficiency along the rims of the scintillators. The quantities a_k are relatively small for the presented set up: $a_2 = 1.032$ and $a_4 = 1.113$.

Prior to the measurements on Rb^{86} two correlations have been investigated for test purposes:

- in a first step the well known $\gamma\gamma$-correlation of Co^{60} has been determined with high accuracy:

Tab. 1. Anisotropy coefficients of the $\gamma\gamma$-angular correlation for Co^{60}.

	Experiment	Theory
A_2	0.1010 ± 0.0011	0.1020
A_4	0.0092 ± 0.0007	0.0091

- secondly the $\beta\gamma$-correlation of Co^{60} (which should be isotropic within the accuracy of the measurement) has been investigated.

Tab. 2. Anisotropy coefficients of the βγ-angular correlation for Co^{60}

	Experiment		Theory	
$\bar{W}$	A_2	A_4	A_2	A_4
1.27	-0.00010±0.00019	0.0±0.00012	$<5\ 10^{-5}$	$<10^{-7}$

This up to now most accurate experimental result agrees with previously published values.

II. 2. The βγ circular polarization correlation measurement

This type of investigation implies, in addition to an energy dependent βγ angular correlation measurement, the analysation of the degree of circular polarization for the γ-rays. As a result, the development of the angular correlation in a series of Legendre polynomials contains also odd coefficients, i.e. A_1 and A_3. Explicitly the circular polarization of the γ-rays reads |30,32|

$$P_\gamma = - \frac{A_1 P_1(\cos\theta) + A_3 P_3(\cos\theta)}{1 + A_2 P_2(\cos\theta) + A_4 P_4(\cos\theta)} = A \frac{v}{c} \cos\theta \qquad (8)$$

The quantity P_γ is determined as usual by employing the polarization dependence of the Compton scattering cross section on magnetized iron |37,38|.

The principle experimental layout is shown in figs. 6 and 7. Again, four β-detectors and two γ-detectors are used, so that systematic errors can be largely reduced |39|.

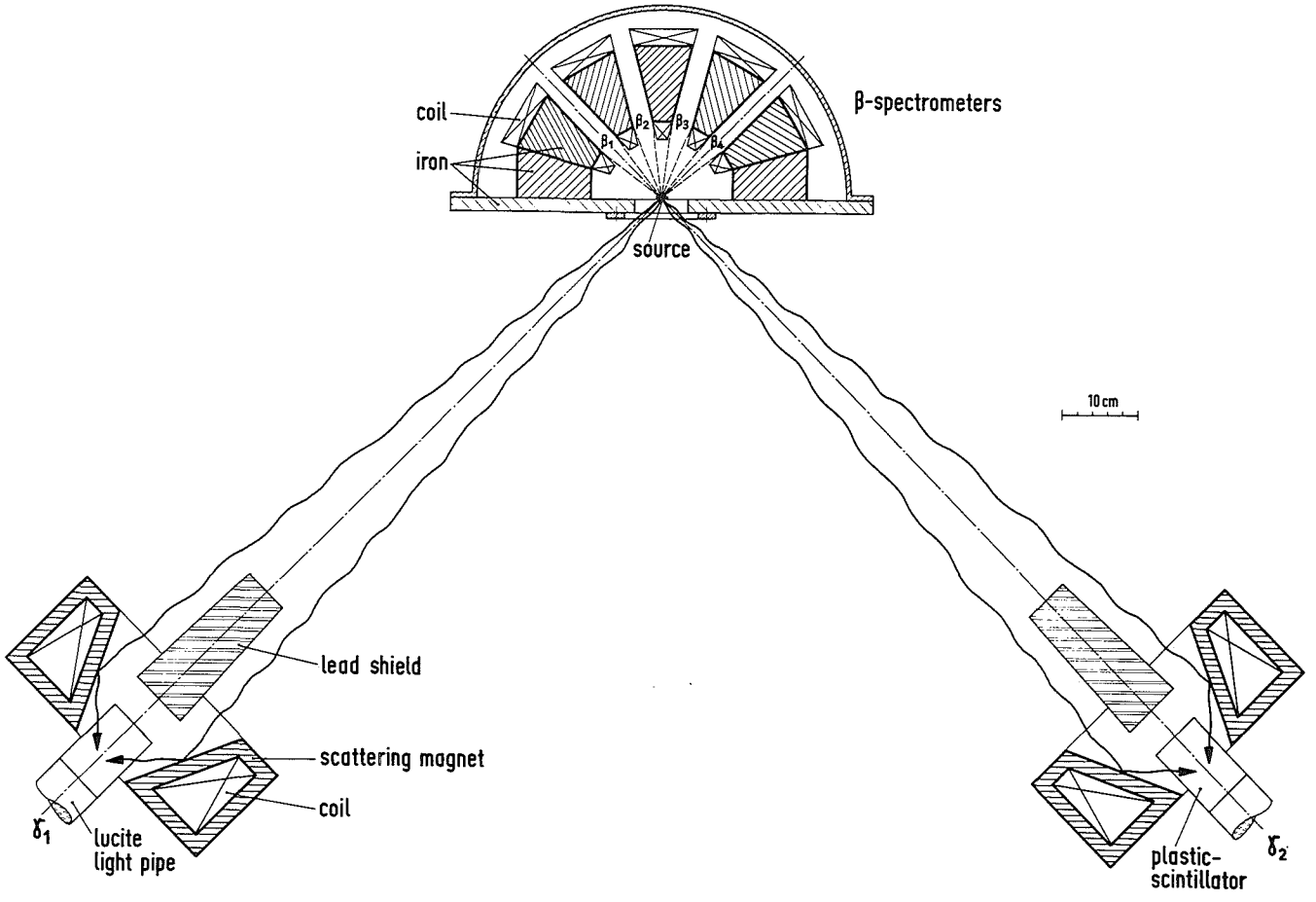

Fig. 6. Experimental arrangement for the measurement of the circular polarization correlation.

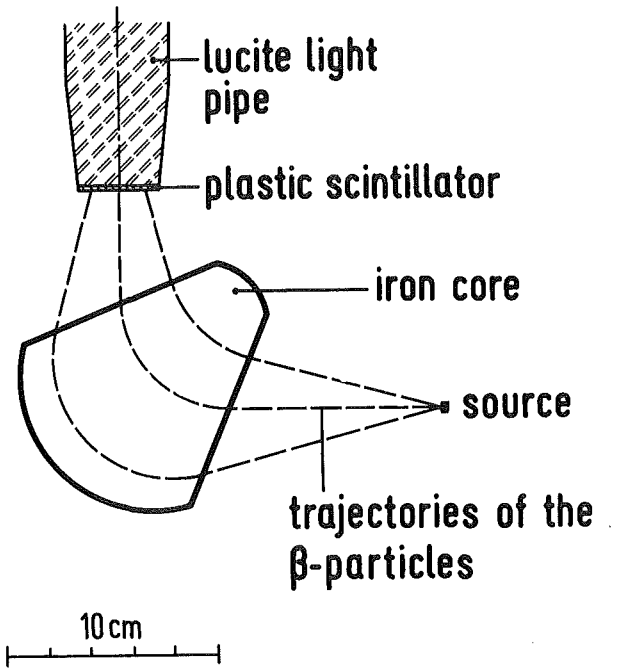

Fig. 7. Vertical cross section through one of the β-spectrometers

The low efficiency for γ-detection because of small accepted solid angles and the preceding Compton scattering process suggested an intensive source strength and therefore a discrimination against the high β-rate by sector field slit spectrometers. Their transmission of about 1% and a momentum resolution of about 20% was considered sufficient for the purpose in question.

The Compton polarimeters have been placed in a comparatively large distance (about 1 m) from the source position.

This has the following advantages:

- fairly precise angle definition
- possible use of the cylindrically symmetric Compton spectrometers (no correction on linearly polarized γ-rays necessary, see App. B)
- no influence of the fringing magnetic field of the polarimeters on the β-spectrometers.

The quantity taken from the measurement is

$$\delta = \frac{K_{ij}^{+} - K_{ij}^{-}}{K_{ij}^{+} + K_{ij}^{-}} \quad , \tag{9}$$

where K_{ij}^{-} and K_{ij}^{+} are the coincidence counting rates for the two magnetization directions. The indices i and j refer to the relevant β and γ counters, respectively. This relative change in the counting rate is related to the circular polarization of the γ-quanta by

$$\delta = f \, P_{\gamma} \cdot \left\langle \frac{d\sigma_c}{d\sigma_o} \right\rangle \tag{10}$$

where f is the fraction of polarized electrons in magnetized iron (≈0.08) and $d\sigma_c/d\sigma_o$ (≈ 0.5 for 1 MeV γ-quanta) the ratio of the polarization dependent to polarization independent Compton scattering cross section. The relative change in the counting rate δ is, therefore, typically smaller than 1 percent.

The chosen geometry allows the simultaneous measurement of 8 coincidence rates where each two rates are attributed to the same relative angle.

From the point of view of the counting rate evaluation the situation is similar to that one described in chapter II.1. for the angular correlation measurement: The geometrical exchange of the two γ-counters there corresponds to the change of magnetization of the two analyzing magnets in front of the γ-counters here. But, this is only true as long as the direction of magnetization in both analyzers is either directed towards or away from the source position. Since the influence of the fringing field of the analyzing magnets on the sector field β-spectrometers introduced some problems in this experiment the magnetization of the analyzing magnets had been chosen in reverse direction; thus their fringing field was minimized. As a consequence the counting rate evaluation had to be carried out straight-forward in the usual manner*)

---

*) In case of similar magnetization of the analyzers it is advantageous to introduce ratios Q of suitable coincidence rates (es evaluated in chapter II.1.:

$$Q_1^{\pm} = \left(\frac{K_{41} \cdot K_{12}}{K_{11} \cdot K_{42}}\right)^{\pm} \quad \text{or} \quad Q_2 = \left(\frac{K_{31} \cdot K_{22}}{K_{21} \cdot K_{32}}\right)^{\pm}$$

where the + or - sign refers to the magnetization direction of the analyzers.

The ratios Q^+/Q^- can be developed in a series resulting for the given arrangement in

$$Q_1^+/Q_1^- \approx 1 - 4\delta(180^\circ) + 4\delta(90^\circ) \quad \text{and}$$

$$Q_2^+/Q_2^- \approx 1 - 4\delta(150^\circ) + 4\delta(120^\circ)$$

Introducing the relevant relations for δ and P_γ (see eqs. (8) and (10)) it is possible to determine A_1 and A_3 if the coefficients A_2 and A_4 are taken from angular correlation measurements.

If the two analyzers are magnetized in reverse directions (as in the experiment reported here) the quantities Q read

$$Q_3^{\pm} = \left(\frac{K_{41} \cdot K_{42}}{K_{11} \cdot K_{12}}\right) \quad \text{and} \quad Q_4^{\pm} = \left(\frac{K_{31} \cdot K_{32}}{K_{21} \cdot K_{22}}\right)$$

The ratios Q^+/Q^- then result in

$$\frac{Q_3^+}{Q_3^-} \approx 1 - 4\delta(180^o) + 4\delta(90^o) \text{ and}$$

$$\frac{Q_4^+}{Q_4^-} \approx 1 - 4\delta(150^o) + 4\delta(120^o).$$

While for Q_1 and Q_2 the detection efficiences of the β- and γ-counters cancel, this is not true any more for the ratios $Q_3^{\pm}$ and $Q_4^{\pm}$ where only the γ-counter efficiencies drop out. Evaluation of quantities $Q_1^{\pm}$ and $Q_2^{\pm}$ for the case of reverse magnetization directions of the two analyzers results in a series with no terms linear in δ.

Details for the data evaluation in such types of experiments are given in ref. |38|.

---

leading to values for P_γ as a function of the angle θ between the directions of the momenta for β particles and γ-quanta, respectively. A direct comparison of the observed values of P_γ with the theory has to be preferred to a separate treatment of A_1 and A_3 anyway, because of the considerable statistical uncertainties in this kind of measurement. In the latter case one has, in addition, to rely on values for A_2 taken from seperate experiments.

In principle solid angle corrections have to be considered similar to the procedure applied in the angular correlation case. No particular emphasis was lead, however, on these corrections here because of the small accepted angles.

The effects of β multiple scattering were estimated according to Frankel |33,34; see also 38| to contribute in the average less than 10% to the final result. These calculations have been considered suffiently accurate from the point of view of the overall statistical error. The justification for not applying the more detailed but also time consuming Monte Carlo method described in appendix A has been proved for some especially chosen experimental values.

The influence of β backscattering in the source backing has been estimated to contribute less than 1% with respect to the final result.
The analyzing efficiency for the polarimeter is $f \cdot \langle \frac{d\sigma_c}{d\sigma_o} \rangle$.
The quantity f has been taken from the saturation magnetization to be $7.05 \cdot 10^{-2}$. The ratio $\langle d\sigma_c/d\sigma_o \rangle$ has been calculated for the special geometry of magnet and detector by numerical integration. The method is presented in details in refs. |37,38|.

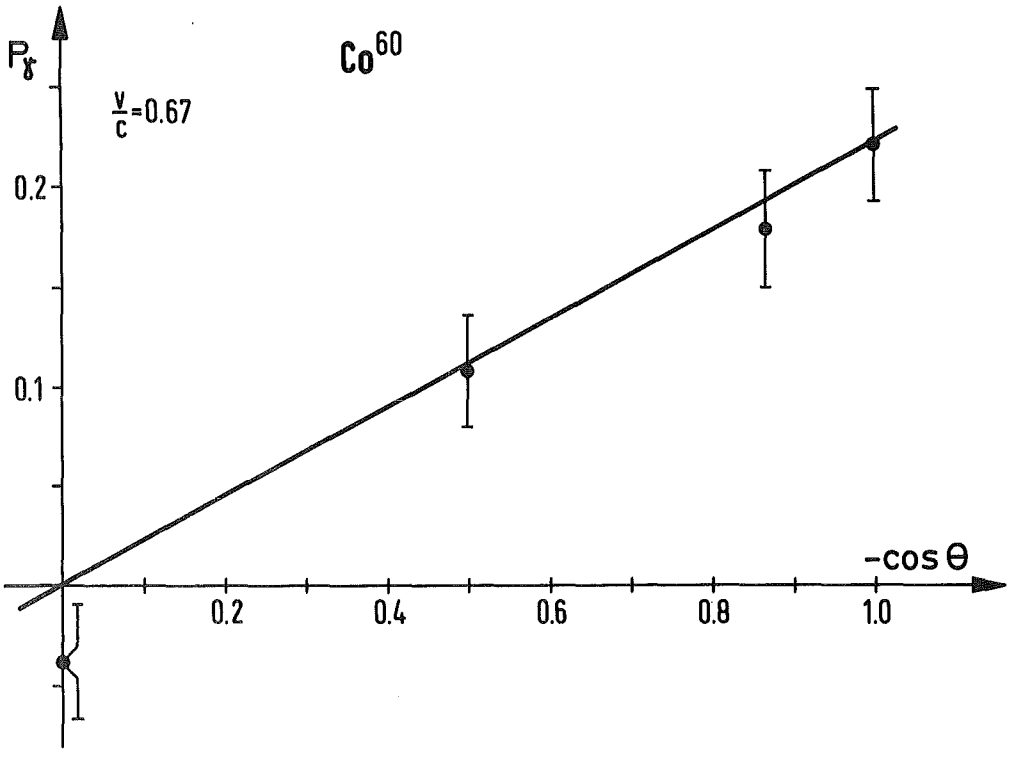

Fig.8. Experimental result for the β-γ circular polarization correlation measurement on Co^{60} (P_γ = circular polarization; θ = angle between β and γ). The theoretical curve is also shown.

The calculated efficiency has been supported by an absolute calibration measurement employing the βγ-transitions in Co^{60}. The results shown in fig. 8 compare favourably with the expectation for $P_\gamma = -\frac{1}{3}\frac{v}{c}\cos\theta$ for the allowed β transition. In fig. 8 P_γ is represented by a straight line with $\frac{v}{c} = 0.67$ in this measurement.

II. 3. Source preparation

Natural Rb was irradiated as RbCl in the Karlsruhe reactor FR2 with a neutron flux of $9 \cdot 10^{13}$ neutrons/$cm^2 \cdot s$. Four weeks' irradiation times were chosen leading to activities between 4 and 6 Ci/g. The activated compound was evaporated on mica foils (0.74 mg cm^{-2}) in areas 4 to 6 mm diameter. The source surface density varied between 0.25 and 5 mg cm^{-2} for the βγ angular correlation measurement and 1.2 and 8.6 mg cm^{-2} for the βγ circular polarization correlation measurement. For the angular correlation investigations especially at low energies a carrier free sample was used which has been produced by the mass separator of the Cyclotron Laboratory. The hygroscopic RbCl sources finally needed a cover. This was supplied by a thin evaporated gold foil of negligible surface density. This cover, in addition, provided electrical conductivity. The evaporation method is certainly most advantageous if one aims a homogeneous source layer. The homogeneosity is, however, required for reliable multiple and backscattering corrections.

III. Results

III. 1. βγ angular correlation measurement

The anisotropy coefficients A_2 and A_4 taken from the measurements are listed in Table 3 for an energy range W = 1.256 through W = 2.278 in natural units. All corrections discussed at length in chapter 2 have been applied to the data. Statistical and the correction dependent systematic errors are listed separately.

Tab. 3. Experimental results of the βγ angular correlation measurement on Rb^{86} (W= β-energy; A_2,A_4=anisotropy coefficients)

W	A_2	A_4
1.256	0.0632 ± 0.0018 (0.0022) 0.0029	0.0030 ± 0.0014 (0.0007) 0.0016
1.372	0.0795 ± 0.0029 (0.0017) 0.0034	0.0059 ± 0.0021 (0.0005) 0.0022
1.489	0.1062 ± 0.0026 (0.0014) 0.0029	0.0052 ± 0.0018 (0.0004) 0.0019
1.605	0.1223 ± 0.0028 (0.0012) 0.0030	0.0022 ± 0.0020 (0.0005) 0.0021
1.722	0.1377 ± 0.0013 (0.0056) 0.0058	-0.0006 ± 0.0010 (0.0022) 0.0024
1.836	0.1573 ± 0.0023 (0.0070) 0.0074	0.0017 ± 0.0016 (0.0021) 0.0027
1.951	0.1845 ± 0.0033 (0.0079) 0.0086	-0.0005 ± 0.0023 (0.0029) 0.0037
2.065	0.1952 ± 0.0044 (0.0082) 0.0094	0.0026 ± 0.0031 (0.0030) 0.0043
2.174	0.2136 ± 0.0040 (0.0090) 0.0099	-0.0047 ± 0.0028 (0.0038) 0.0047
2.278	0.1976 ± 0.0119 (0.0064) 0.0135	0.0023 ± 0.0087 (0.0032) 0.0092

The results are consistent with some published data |10,11,13|. This is not necessarily true for several other published values |3,8,9,12,15|. A remarkably small error is characteristic for the results reported here, especially for the low energy range.

III. 2. βγ circular polarization correlation measurements.

The polarization P_γ for an average energy $\bar{W} = 1.74$ is listed in Table 4 for four angles. Again, statistical and systematic errors are separately quoted. For details see ref. |39|. Within the errors the results are in agreement with recently published data |7,17,18,19| but differ from the values quoted in |11,16|.

Tab. 4. Experimental results of the βγ circular polarization correlation measurement on Rb^{86} for an average β-energy of $W = 1.74$ (θ = angle between β and γ; P_γ = polarization)

θ	P_γ
90°	$0.038 \pm \begin{matrix} 0.032 \\ (0.003) \\ \hline 0.032 \end{matrix}$
120°	$-0.059 \pm \begin{matrix} 0.035 \\ (0.004) \\ \hline 0.035 \end{matrix}$
150°	$-0.039 \pm \begin{matrix} 0.029 \\ (0.003) \\ \hline 0.029 \end{matrix}$
176°	$-0.027 \pm \begin{matrix} 0.034 \\ (0.002) \\ \hline 0.034 \end{matrix}$

IV. Analysis

IV. 1. Theoretical remarks

Since the ground state of Rb^{86} and the first excited state of Sr^{86} cannot be interpreted by means of the simple shell model a more complete picture is required.

Fortunately Rb^{86}, representing a nearly semi magic configuration, ranges amongst nuclei that have been extensively considered theoretically. Talmi |40| and Shlomo and Talmi |41| deal in details with the structure of semi magic nuclei while Kitching et al. |42| explicitly calculate the configurations for strontium isotopes employing effective interaction between $1g_{9/2}$ and $2p_{3/2}$ states. For Sr^{86} the latter paper leads for the first excited 2^- state to $g_{9/2}^{-2}$ and pure seniority 2. This result leaves unsatisfied since the experimental data for the β decay of Rb^{86} strongly favour the presence of matrix elements of rank 0 and 1. Wahlborn |1| already pointed out to the necessity to include collective effects. This unified model has been elaborated and applied to several odd A strontium isotopes from Sr^{89} through Sr^{83} by Kitching |43|. Assuming weak coupling of quasi particle states observed in the N = 49 nuclei to vibrations of the neighbouring even cores he obtained some improvement over earlier shell model calculations. In a microscopic analysis of shell model configurations for strontium isotopes Ogawa |44| employs a proton-neutron configuration $\pi(2p_{1/2}, 2p_{3/2}, 1f_{5/2})^{-2}\ \nu(1g_{9/2})^{-(50-N)}$. The lowest 2^+ first excited state of Sr^{86}, which has been regarded throughout as a $(g_{9/2})_n^{-2}$ state, is well reproduced including the proton excitations. It is, according to these calculations composed of $|J_p = 0^+\ \ J_n = 2^+;\ J = 2^+>$ and $|J_p = 2^+\ \ J_n = 0^+;\ J = 2^+>$ states with nearly equal weights.

In the following we intend to interpret our experimental results in the framework of weak coupling of shell model states to vibrational states.

The Hamiltonian which describes the single particle motion and the collective motion simultaneously is of the form

$$H = H_{sp} + H_{coll} + H_{int} \cdot \qquad (11)$$

Excellent reviews on this model can be found in refs. |45,46|.

Taking the lowest order pattern we couple the holes to the collective quadrupole $R^{\pi} = 2^{+}$ vibrational excitation. If H_{int} is weak one can treat $H_{sp} + H_{coll}$ as the unperturbed Hamiltonian. We denote the single particle wave function by $|J>$ and the latter by $|NR>$. The solution of $H_{sp} + H_{coll}$ with angular momentum I is then $|J'\ NR;\ I>$.

The basic matrix element associated with the coupling

$$<J',12;\ I\ |H_{int}|\ J,OO;\ I> \qquad (12)$$

describes a process involving the emission or absorption of a vibrational quantum.

The physical state vectors of angular momentum I can be written as *)

$$|I> = a_o|J,OO;\ I> + \sum_{J'} a_{J'}|J',12;\ I>. \qquad (13)$$

The coefficient of the eigenvectors may be evaluated considering the matrix element of eq.(12) by means of the standard procedures such as diagonalization or perturbation calculations. The idea of the present work is to propose the eigenvectors which might describe the beta decay experiments and find the coefficients by fitting them to the theoretical expressions.

---

*) A similar concept was developed by Wahlborn |1|.

The wave functions of eqs. (1) and (3) lead to the single-particle transition $\nu g_{9/2} \rightarrow \pi f_{5/2}$, which allows only matrix elements of rank 2 and higher orders. Such a description could never reproduce the experimental results displayed in figs. 9a-9d, where also the unique prediction is presented. As it was commented in the introduction, nuclear matrix elements of rank 0 and 1 should play an important role in the interpretation of this transition.

The idea is to suggest a set of eigenvectors which allow matrix elements of rank 0 and 1. The basis vectors of the form $|J',12;\ I>$ should be built up taking into account the neighbouring shell levels. Wahlborn |1| has presented a detailed discussion on this problem. He suggested that the following neutron levels

$$j_\nu = {}^{2}d_{5/2},\ {}^{1}g_{7/2},\ {}^{2}d_{3/2}, \qquad (14)$$

may be coupled to the proton hole $j_\pi = {}^{1}f^{-1}_{5/2}$ leading to the angular momentum J', and that the proton levels

$$j_\pi = {}^{1}f_{7/2},\ {}^{1}h_{11/2}, \qquad (15)$$

may be coupled to the neutron hole $j_\nu = {}^{1}g^{-1}_{9/2}$ also resulting in the angular momentum J'.

From the study of the single particle levels one can say that the admixtures of neutron states of eq. (14) must be more important than the proton admixtures presented in eq. (15).

Bearing in mind the discussion mentioned above we propose the following wave functions:

a) for the ground state of Rb^{86}

$$
\begin{aligned}
|Rb^{86}; 2^-\rangle = a_o \Big| \Big[(\nu g_{9/2})^{-1}_{9/2} \quad (\pi f_{5/2})^{-1}_{5/2} \Big] \, 2^-, 00; 2^-\rangle \\
+ a_1 \Big| \Big[(\nu g_{9/2})^{-1}_{9/2} \quad (\pi f_{5/2})^{-1}_{5/2} \Big] J'_1, 12; \, 2^-\rangle \\
+ a_2 \Big| \Big[(\nu g_{9/2})^{-2}_{0} \quad (\nu d_{5/2})^{1}_{5/2} \quad (\pi f_{5/2})^{-1}_{5/2} \Big] \, J'_2, 12; \, 2^- \rangle \\
+ a_3 \Big| \Big[(\nu g_{9/2})^{-2}_{0} \quad (\nu g_{7/2})^{1}_{7/2} (\pi f_{5/2})^{-1}_{5/2} \Big] \, J'_3, 12; \, 2^- \rangle \\
+ a_4 \Big| \Big[(\nu g_{9/2})^{-2}_{0} \quad (\nu d_{3/2})^{1}_{3/2} \quad (\pi f_{5/2})^{-1}_{5/2} \Big] \, J'_4, 12; \, 2^-\rangle ;
\end{aligned}
\tag{16}
$$

b) for the first excited state of Sr^{86}

$$
\begin{aligned}
|Sr^{86}; \, 2^+\rangle = b_o \Big| \Big[(\nu g_{9/2})^{-2}_{2} \Big] 2, 00; \, 2^+\rangle \\
+ b_1 \Big| \Big[(\nu g_{9/2})^{-2}_{0} \Big] 0, 12; \, 2^+\rangle \, .
\end{aligned}
\tag{17}
$$

It is important to mention that the wave functions given by eqs. (16) and (17) are not complete. We are, therefore, able to find only the relative intensity of these compounds. For example

$$
\Big| \Big[(\nu g_{9/2})^{-1}_{9/2} \, , \, (\pi p_{3/2})^{-1}_{3/2} \Big] \, J', 12; \, 2^-\rangle \tag{18}
$$

may also be an eigenvector for $|Rb^{86}; \, 2^-\rangle$, but its matrix element corresponds to the single-particle transition $\nu g_{9/2} \rightarrow \pi p_{3/2}$ and gives rise to matrix elements at least of rank 3. Consequently, its influence to the theoretical expressions is extremely weak, and we are not able to say

anything about its relative contribution from beta decay analysis.

In order to obtain the coefficients a_i and b_f the experimental data were fitted to the theoretical expressions for the observables.
For instance, if we introduce also the proton admixtures such as

$$\left|\left[(\nu g_{9/2})^{-1}_{9/2} \quad (\pi f_{7/2})^{-1}_{7/2}\right] J',12;\ 2^-\right> \qquad (19)$$

then the number of free parameters is enlarged and the selectivity of the fitting test is automatically decreased.

IV. 2. Method of the analysis

The method for the extraction of the coefficients a_i and b_f is based on the minimization of the χ^2_T function, defined as

$$\chi^2_T = \sum_{k=1}^{n} \chi^2(k), \qquad (20)$$

with

$$\chi^2(k) = \sum_{i=1}^{N(k)} \left\{ \left| Q^k_{th}(i) - Q^k_{exp}(i) \right| / \Delta Q^k_{exp}(i) \right\}^2 \qquad (21)$$

where n is the number of the beta observables taken into account (for example $C_\beta(W)$, $A_K(W)$, $P_\gamma(\theta)$, $\delta(W)$, etc.); $N(k)$ is the total number of experimental values of the observable k; $Q^k_{exp}(i)$ and $\Delta Q^k_{exp}(i)$ are the experimental values of the observable k and its error, respectively; and $Q^k_{th}(i)$ is the corresponding theoretical value. The criterion adopted for accepting some particular minimum is to require the condition

$$\frac{\chi^2(k)}{N(k)} \lesssim 1, \qquad (22)$$

for all k, i.e. every observable separately. When this condition is not satisfied the results of the analysis are incorrect (see. ref. |27|).

The minimization procedure was carried out with the aid of the package of subroutines MINUITS, provided by CERN.

The parameters a_1, a_2, a_3, a_4 and b_1 were taken as independent. The other two a_o and b_o were calculated from the normalization conditions

$$\sum_i a_i^2 = 1 \quad \text{and} \quad \sum_f b_f^2 = 1. \qquad (23)$$

This is only a normalization in our basis space, it is not absolute.

IV. 3. Data and Formulae used in the analysis

The following experimental data were analysed:

a) Spectrum shape factor $C_\beta(W)$. The reliable and for a fit-procedure suitably published results reported by Daniel et al. |6| were considered.
b) Beta-gamma directional correlation coefficients $A_2(W)$. Our own experiment |28| was taken into account*).
c) Beta-gamma circular polarization as a function of energy $\delta(W)$. The data published by Bosken et al. |19| were included.
d) Beta-gamma circular polarization as function of angle $P_\gamma(\theta)$. Our own measurement |39| was taken into account.

The formulae used for the calculations of the observables were presented in ref. |32|. They may be written in terms of the quantities $M_K(k_e,k_\nu)$ and $m_K(k_e,k_\nu)$, where K is the tensorial rank of the involved β-operators and k_e and k_ν are the electron and the antineutrino quantum numbers. The expressions for $M_K(k_e,k_\nu)$ and $m_K(k_e,k_\nu)$ have been given in a former work |47|.

*) The theoretical predicitions for A_4 are, irrespective of the used wave functions, consistently $\lesssim 5 \cdot 10^{-5}$. Since the experimental accuracy in this investigation is of the order $2 \cdot 10^{-3}$, it is not practicable to employ this quantity for a fit.

The Fermi- and other Coulomb functions (μ_1, λ_2, Λ_1 etc.) have been calculated employing the computer routines worked out for the tables (III) of Behrens and Jänecke |32|.
For the present analysis only terms in the lowest order were considered, the corresponding formulae are listed in Table 4 of ref. |47| where a thorough discussion about the higher order terms was also done.

To carry out the analysis considering only lowest order terms was justified since several calculations of the higher order terms proved that their contribution is in this case completely negligible.

For the evaluation of $\delta(W)$ one must be careful because the experimentally determined coefficients ε_1, ε_2 and ε_3 should be taken into account as it was pointed out by Bosken et al. |19|.

The calculation of the single particle matrix elements was performed with the formulae given in Table 7 of ref. |47|. The many particle configurations including collective core states are then given as linear combinations of recoupling coefficients and reduced single particle matrix elements. Explicitely, for transitions within equal phonon states, the formula for the form factor coefficients reads:

$$(-1)^{K-L}\, F^{N}_{KLs}\,(k,m,n,\rho) =$$

$$(-1)^{I_i+1} \sum_{J'_f\, J'_i,\, R} a(J'_i,\, I_i^{(n)},\, I_i^{(p)}, R) \cdot b(J'_f,\, I_f^{(n)},\, I_f^{(p)}, R) \cdot$$

$$\begin{matrix} I_f^{(n)} & I_i^{(n)} \\ I_f^{(p)} & I_i^{(p)} \\ j_n & j_p \end{matrix}$$

$$\cdot\, (-1)^{J'_f + R + I_f^{(n)} - I_i^{(n)} - j_p} \cdot \left[(2I_i + 1)(2I_f + 1)\right]^{1/2}$$

$$\cdot \left[(2I_i^{(n)} + 1)(2I_f^{(p)} + 1)(2J'_i + 1)(2J'_f + 1)\right]^{1/2}$$

$$\cdot\sqrt{N^{(n)}}\,\sqrt{N^{(p)}+1}\begin{Bmatrix} J_f' & I_f & R \\ I_i & J_i' & K \end{Bmatrix}\left[\left[j_n^{\,N^{(n)}-1}(\alpha_f^{(n)}\ I_f^{(n)})\, j_n\ I_i^{(n)} \right\}\right.$$

$$\left. j_n^{N^{(n)}} \cdot \alpha_i^{(n)}\ I_i^{(n)}\right]$$

$$\cdot\left[j_p^{\,N^{(p)}}(\alpha_i^{(p)}\ I_i^{(p)})\ j_p\ I_f^{(p)} \right\}\ j_p^{\,N^{(p)}+1} \cdot \alpha_f^{(p)}\ I_f^{(p)}\right]$$

$$\cdot\begin{Bmatrix} I_f^{(n)} & I_f^{(p)} & J_f' \\ I_i^{(n)} & I_i^{(p)} & J_i' \\ j_n & j_p & K \end{Bmatrix}\left[M^N_{KLs}\ (k,m,n,\rho)_{s.p.} \right]_{j_n,j_p} \qquad (24)$$

where the neutrons and protons with angular momentum j_n and j_p couple to $I_i^{(n)}$, $I_f^{(n)}$, $I_i^{(p)}$ and $I_f^{(p)}$, respectively. $N^{(n)}$ and $N^{(p)}$ are the number of neutrons and protons, respectively, in the initial state. The $\left[\,|\,\}\right]$ are fractional parentage coefficients.

IV. 4. Results of the analysis

The determination of the coefficients was achieved under various assumptions. For the radial wave functions (a) the harmonic oscillator potential and (b) the Woods-Saxon potential were considered. In each case the protons and neutrons were coupled in two different ways to give J'.

The solutions for all the cases were found in the regions quoted in Table 5. A glance at this table indicates that a very small admixture of a_2 and a_3 in $|Rb^{86};\ 2^-\rangle$ is sufficient to describe the beta experiments. It is interesting to point out that the admixture of $\nu d_{5/2}$ is more important than the corresponding $\nu g_{7/2}$ as it is expected from the single-

particle level scheme given in fig. 1.

The first excited 2^+-level of Sr^{86} is found to consist of approximately equal contributions of the configurations with two holes in the $g_{9/2}$ shell and seniority 2 and seniority 0, respectively, the latter coupled to a one phonon excited state. This is fully consistent with the theoretical result in microscopic consideration by Ogawa |44| as mentioned in chapter IV.1.

The application of the wave functions evaluated in this paper to calculations of the magnetic dipole and electric quadrupol moments for the ground state of Rb^{86} will be discussed in a forthcoming paper.

Tab. 5. Coefficients for the wave functions of $|Rb^{86}; 2^->$ and $|Sr^{86}; 2^+>$ extracted from the experimental data.

Coefficient	Harmonic Oscillator			Woods - Saxon	
	J' = K		J' = $\|j_n - j_p\|$	$a_2 = a_4 = 0$	
	$a_4 = 0$	$a_2 = 0$	$a_2 = a_4 = 0$	J' = K	J' = $\|j_n - j_p\|$
a_o	0.91 - 0.99	0.92 - 0.99	0.94 - 0.997	0.978 - 0.996	0.971 - 0.997
a_1	0.00 - 0.36	0	0	0	0
a_2	0.13 - 0.40	0.13 - 0.37	0.15 - 0.32	0.08 - 0.21	0.07 - 0.24
a_3	0.02 - 0.07	0.02 - 0.07	-0.03 - -0.01	-0.007 - -0.003	-0.032 - -0.011
a_4	0	-0.09 - -0.02	0	0	0
b_o	0.56 - 0.91	0.56 - 0.89	0.58 - 0.84	0.56 - 0.87	0.53 - 0.89
b_1	0.42 - 0.83	0.45 - 0.83	0.54 - 0.81	0.50 - 0.83	0.46 - 0.85

Tab. 6. Form factor coefficients which correspond to wave functions of Tab.5.
a) Harmonic oscillator (a_o = 0.929, $a_1=a_4=0$, $a_2=0.364$, $a_3=0.064$, b_o = 0.891, b_1 = 0.454)

b) Woods Saxon (a_o= 0.978, $a_1=a_4=0$, $a_2=0.207$, $a_3=-0.007$, b_o= 0.864, $b_1=0.504$)

	n	m	ρ	a)	b)
$A_{F^o_{ooo}}(k_e = 1)$	n	m	0	0.0499	0.0394
$A_{F^o_{o11}}(k_e = 1)$	n	m	0	0.200	0.0896
	1	1	1	0.216	0.0896
$V_{F^o_{110}}(k_e = 1)$	n	m	0	-0.0729	-0.0069
	1	1	1	-0.0860	-0.0055
$V_{F^o_{101}}(k_e = 1)$	n	m	0	0.0105	0.0023
$A_{F^o_{111}}(k_e = 1)$	n	m	0	-0.104	-0.0689
	1	1	1	-0.105	-0.0701
$A_{F^o_{211}}(k_e = 1)$	n	m	0	-1.261	-1.312
log ft				6.85	6.79

IV. 5. Theoretical estimation in the weak coupling model.

A rough calculation for these coefficients was performed by means of perturbation theory. The coefficient $a_{J'}$ can be written in first order of the coupling constant as (see ref.|46|).

$$a_{J'} = - \frac{\langle J',12;\ I\ |H_{int}|J,00;\ I\rangle}{\hbar\omega_2 + E_{J'} - E_J} \qquad (25)$$

where $\hbar\omega_2$ is the phonon energy, $E_{J'}$ and E_J were approximated to the single-particle energy of the neutrons $\nu d_{5/2}$ or $\nu g_{7/2}$, and the single-particle energy of $\nu g_{9/2}$, respectively.

In a first approximation the interaction of particles (holes) with the oscillating core is given by |46|

$$H_{int} = \mp \sum_i k_\lambda(r_i) \sum_{\lambda\mu} \alpha^*_{\lambda\mu}\ Y^{(i)}_{\lambda\mu}\ (\theta,\phi), \qquad (26)$$

where $k_\lambda(r_i)$ is the strength and radial dependence of the interaction for the i-th particle (hole). The quantities $\alpha^*_{\lambda\mu}$ are the deformation parameters. The $Y^{(i)}_{\lambda\mu}(\theta,\phi)$ are the spherical harmonics to the multipole moments of the particle motion. Finally, (±) refers to the particle-surface and hole-surface interaction, respectively.

The radial factor $k_\lambda(r)$ is taken as

$$k_\lambda(r) = r\left[\frac{dV(r)}{dr}\right], \qquad (27)$$

here V(r) is the single particle potential.
The results are,

$$\begin{aligned}
a_{J'=0}(d_{5/2}) &= 0.323 & a_{J'=1}(d_{5/2}) &= 0.386 \\
a_{J'=1}(g_{7/2}) &= 0.034 & a_{J'=2}(g_{7/2}) &= 0.037 \qquad (28) \\
a_{J'=1}(d_{3/2}) &= 0 & a_{J'=2}(d_{3/2}) &= 0\ .
\end{aligned}$$

For the radial wave function the Woods-Saxon type was used. The agreement with the extracted coefficients is extremely good, especially if one considers the rough approach used in this evaluation.

In Table 6 the values of the form factor coefficients are listed for a typical set of wave function coefficients and figs. 9a - 9d show the fitting.

IV. 6. Concluding remark

It is important to note that the procedure reported here is an attempt to find directly the nuclear structure from beta decay studies. Most of the former analyses were restricted to find some nuclear matrix elements which explain particular experimental data.

The authors are indebted to Mr. J. Müller for source preparation and Mr. B. Feurer for isotope separation.

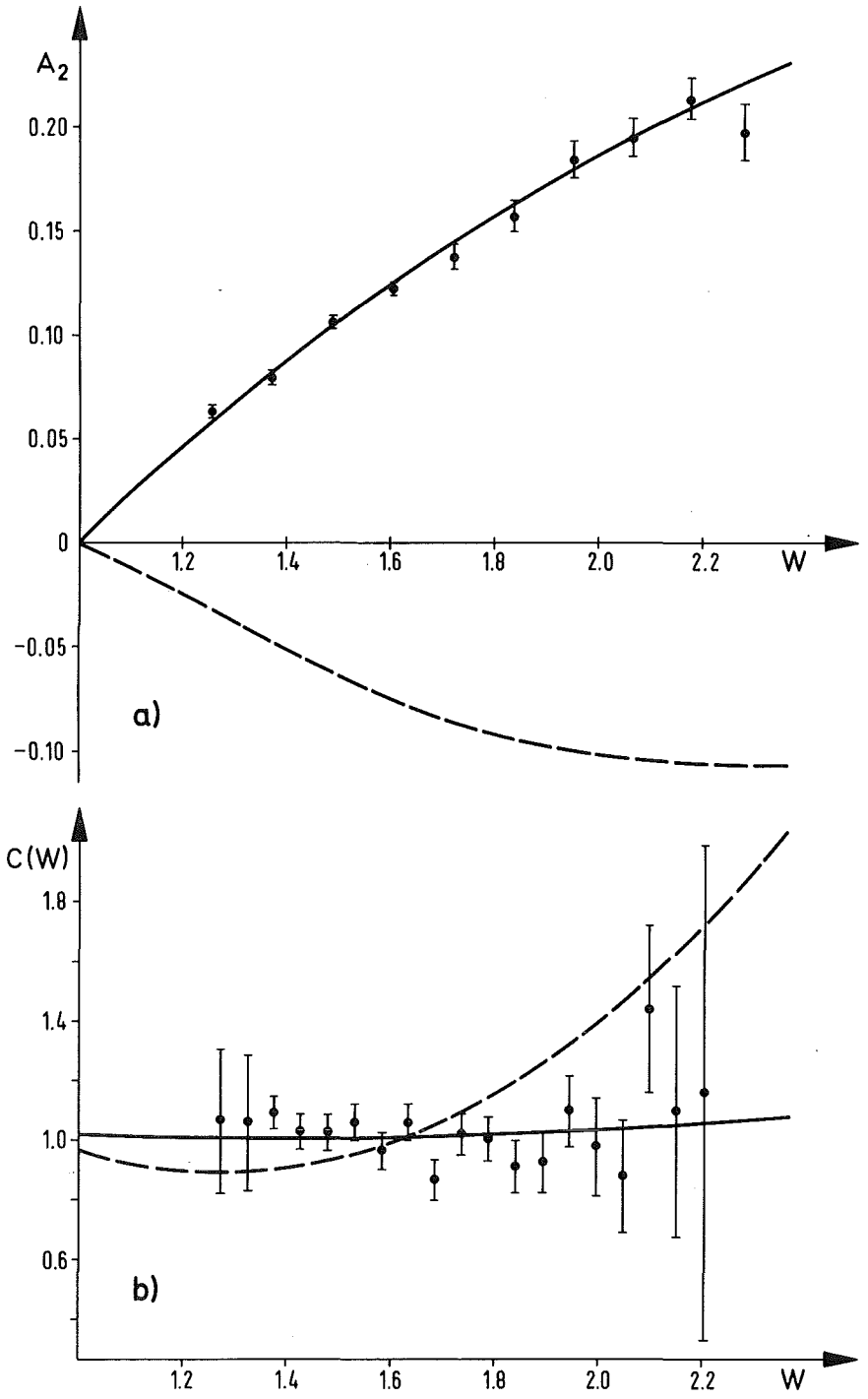

Fig.9. Observables of Rb^{86} (--- simple shell model, — fit)

a) β-γ angular correlation. A_2 as a function of the β energy.

b) shape factor C(W) (from ref. |6|) as a function of the β energy.

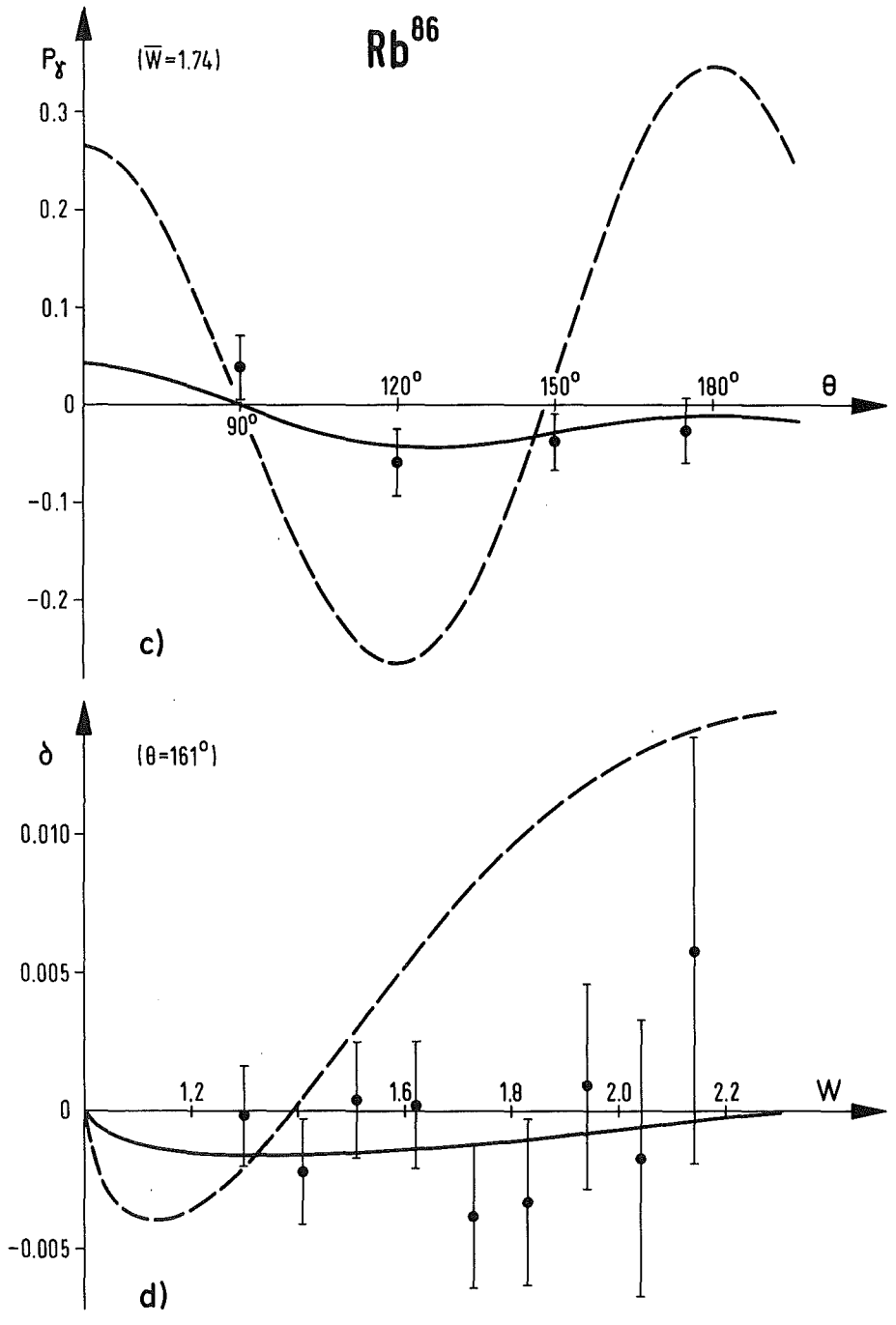

c) β-γ-circular polarization correlation. Polarization P_γ as a function of the angle θ between β and γ.

d) β-γ-circular polarization correlation (from ref. |19|) δ as a function of the β-energy.

Appendix A

The probability for scattering of an electron through an angle α is $F(\alpha)$. If, as in the presented case, the β-detectors are positioned under scalene angles to the area of the source this probability F is also dependent on the azimuthal angle ϕ.

We denote β as the angle of the β-counter axis with respect to direction normal to the source and α,ϕ as the polar and azimuthal angles, respectively, with respect to the direction source-counter. The probability for a particle which starts under the angles α, ϕ, to leave the source under an angle β is defined by $F(\beta, \alpha,\phi)$.

Then a coincidence event between a β particle and a γ quantum has the probability

$$P = d\Omega_\beta \, d\Omega_\gamma \int \omega(\theta) \cdot F(\beta, \alpha, \phi) \sin\alpha \, d\alpha \, d\phi \qquad (A\ 1)$$

with $d\Omega_\beta$ and $d\Omega_\gamma$ as the solid angles accepted by the β- and the γ-counter, respectively, and $\omega(\theta)$ the $\beta\gamma$ correlation for the relevant angle θ; the latter can be written

$$\omega(\theta) = \sum_\ell A_\ell \, P_\ell(\cos\theta) = \sum_\ell \sum_{m=-\ell}^{+\ell} \frac{4\pi}{2\ell+1} A_\ell \, Y_\ell^{m*}(\alpha,\phi) \cdot$$

$$\cdot \, Y_\ell^m(\theta',0) \qquad (A\ 2)$$

where θ' is the angle between β- and γ-counter. With respect to the dependence on α, β and ϕ the scattering probability F is developed in terms of spherical harmonics:

$$F(\alpha,\beta,\phi) = \sum_\ell \sum_{m=-\ell}^{+\ell} \sqrt{\frac{2\ell+1\,(\ell+m)!}{4\pi \quad (\ell-m)!}} \, b_\ell^m(\beta) \, Y_\ell^m(\alpha,\phi) \qquad (A\ 3)$$

Employing the orthogonality relation and combining positive and negative m-values appropriately leads to

$$P(\theta',\beta) = d\Omega_\beta \, d\Omega_\gamma \cdot \sum_{\ell} \sum_{0 \le m \le \ell} A_\ell \cdot B_\ell^m(\beta) \cdot P_\ell^m(\cos\theta') \qquad \text{(A 4)}$$

with

$$B_\ell^m(\beta) = b_\ell^m(\beta) + (-1)^m \frac{(\ell-m)!}{(\ell+m)!} b_\ell^{-m}(\beta)$$

$$= 2 \cdot \frac{(\ell-m)!}{(\ell+m)!} \int F(\beta,\alpha,\phi) \; P_\ell^m(\cos\alpha) \cdot \cos(m\phi) \quad \sin\alpha \; d\alpha \; d\phi$$

$$\text{for } 0 < m \le \ell \qquad \text{(A 5)}$$

$$B_\ell^0(\beta) = \int F(\beta,\alpha,\phi) \cdot P_\ell(\cos\alpha) \; \sin\alpha \; d\alpha \; d\phi \qquad \text{(A 6)}$$

Since an analytic treatment does not seem possible, the scattering distribution has been obtained by Monte Carlo methods. The calculation procedure has been chosen according to Paul and Tatzber |48| .

The program simulates a source of thickness z_o infinitely extended in x- and y-direction. The experience of a single electron is determined by the following random events: After definition of the starting position z, $0 \le z \le z_o$, and the original direction of the flight path, the particle track is determined by the mean free paths and the scattering angles until the particle leaves the source, i.e. $z < 0$ or $z > z_o$.

For final flight path directions within the cone $2\pi \sin\beta \, \Delta\beta$ the start parameters α and ϕ are used to calculate $F(\beta,\alpha,\phi)$.

The Monte Carlo calculation has been performed under the following assumptions:

a) the scattering process happens to be incoherent
b) no scattering occurs on single atomic electrons
c) radiation effects are negligible.

Taking the nuclei as infinitely heavy, assumptions b) and c) imply that the scattered electrons do not suffer energy losses.

It is useful to introduce the scattering cross section analytically. In first order Born approximation this leads to

$$\frac{d\sigma}{d\Omega} = 4\ Z^2\ r_o^2\ E^2\ \frac{[1 - F(q_o)]}{q_o^4} \qquad \text{(A 7)}$$

where $F(q_o)$ is the so-called atomic form factor divided by the atomic number Z. E and p are the energy and momentum of the electron, respectively, $q_o = 2p \sin\theta/2$ is the momentum transfer. r_o denotes the classical electron radius.

Equ. (A 7) has been taken from a survey article by Motz, Olsen and Koch |49|. Using a potential of the form

$$V(r) = \frac{Z \cdot e^2}{r} \sum_{i=1}^{3} a_i \cdot e^{-b_i r} \qquad \text{(A 8)}$$

the cross section reads

$$\frac{d\sigma}{d\Omega} = 4\ Z^2\ r_o^2\ E^2 \left(\sum_{i=1}^{3} \frac{a_i}{b_i^2 + q_o^2} \right)^2; \qquad \text{(A 9)}$$

where the coefficients $a_i = a_i(Z)$ and $b_i = b_i(Z)$ are taken from Bonham and Strand |50|.

Introducing the probabilities $P(\theta',\beta)$ from eq. (A 4) in the quantities Q_i of eq. (5) we obtain the ratios:

Position I

$$Q_1 = \frac{P(90^o,\beta_1) \cdot P(90^o, \beta_2)}{P(45^o,\beta_2) \cdot P(135^o,\beta_1)}$$

$$Q_2 = \frac{P(180^o,\beta_1) \cdot P(180^o,\beta_2)}{P(135^o,\beta_1) \cdot P(135^o,\beta_2)}$$

Position II

$$Q_3 = \frac{P(90^o,\beta_2)^2}{P(135^o,\beta_2)^2}$$

$$Q_4 = \frac{P(180^o,\beta_1)^2}{P(135^o,\beta_1)^2} \qquad \text{(A 10)}$$

where $\beta_1 = 22.5^o$ and $\beta_2 = 67.5^o$

Position III

analog position I, with Q_1 and Q_2 interchanged.

An explicit calculation of eqs. (A 10) allows to express the anisotropy coefficients A_2 and A_4 as function of the Q_i and B_ℓ^m. Actually, for Position I and III A_2 and A_4 appear in a system of two equations of second degree, for position II in two equations of first degree.

Thus, the experimental determination of the Q_i together with the calculable B_ℓ^m leads to the true anisotropy coefficients A_2 and A_4.

Appendix B

Circular polarization analysis of γ-rays after β transitions has predominately been carried out using Compton effect as a tool. In these investigations it is necessary to distinguish between allowed and forbidden β-transitions. While the former leave the residual nucleus in a pure polarized state, the latter transitions include the possibility that the final state after β-decay is also aligned. Consequently, following allowed β-transitions one observes purely circular polarized γ-rays. Radiation emitted after forbidden β-transitions may in addition also show linear polarization.

Taking

$$\omega(\theta,W,\tau) = \frac{1}{S} \sum_{k=\text{even}} B_k(\beta)\, A_k(\gamma)\, P_k(\cos\theta) - \tau \sum_{k=\text{odd}} B_k(\beta)\, A_k(\gamma)\, P_k(\cos\theta) \qquad \text{(B 1)}$$

as the βγ correlation (see, e.g. refs. |31,32|)
then

$$P_\gamma = \frac{\omega(\theta,W,\tau=+1) - \omega(\theta,W,\tau=-1)}{\omega(\theta,W,\tau=+1) + \omega(\theta,W,\tau=-1)} \qquad \text{(B 2)}$$

represents the circular polarization of the γ-radiation.

The differential Compton scattering cross section is

$$\frac{d\sigma}{d\Omega} \sim \frac{d\sigma_o}{d\Omega} + P_\ell \frac{d\sigma_\ell}{d\Omega} + f\, P_\gamma \frac{d\sigma_c}{d\Omega} \qquad \text{(B 3)}$$

where

$\frac{d\sigma_o}{d\Omega}$ is the ordinary (polarization independent) Compton cross section,

$\frac{d\sigma_\ell}{d\sigma}$ and $\frac{d\sigma_c}{d\sigma}$ are the linear and circular polarization dependent terms, respectively,

P_ℓ and P_γ are the relevant degrees of polarization and

f is the fraction of oriented electrons in the scatterer.

$$\Delta = \frac{d\sigma^- - d\sigma^+}{d\sigma^- + d\sigma^+} \qquad \text{(B 4)}$$

with $d\sigma^+$ and $d\sigma^-$ as the scattering cross sections for γ-rays in the respective polarization directions of the electrons in the scatterer
is then

$$\Delta = \frac{f\, P_\gamma \,\langle d\sigma_c/d\sigma_o\rangle}{1 + P_\ell \,\langle d\sigma_\ell/d\sigma_o\rangle} \qquad \text{(B 5)}$$

The circular polarization P_γ has already been expressed in terms of Legendre polynomials in equation (B 2). The linear polarization P_ℓ reads

$$P_\ell(\theta, W, \psi) = \frac{1}{S} \sum_{k=\text{even}} B_k(\beta)\; E_k(\gamma)\; P_k^{(2)}(\cos\theta)\; \cos 2\psi \qquad \text{(B 6)}$$

where ψ is the angle between the electric vector of the radiation and the plane of Compton scattering. $P_k^{(2)}$ is an associated Legendre polynomial and

$$E_k(\gamma) = \Big\{(-1)^{\sigma_L} \cdot F_k(L\ L\ j_2 j_1)\, \frac{2k(k+1)L(L+1)}{k(k+1)-2L(L+1)} + 2\delta(-1)^{\sigma_{L'}} \cdot$$

$$\cdot F_k(L\ L'\ j_2 j_1) \cdot (L'-L)(L'+L+1) + \delta^2 (-1)^{\sigma_{L'}} \cdot F_k(L'\ L'\ j_2 j_1)$$

$$\frac{2k(k+1)\ L'\ (L'+1)}{k(k+1)-2L'(L'+1)}\Big\}\ \frac{(k-2)!}{(k+2)!} \qquad \text{(B 7)}$$

with

σ_{L_γ} = + 1 for electric $(2)^L$-pole radiation

σ_{L_γ} = - 1 for magnetic $(2)^L$-pole radiation.

j_1 = angular momentum of the initial state

j_2 = angular momentum of the final state after the γ transition.

δ = mixing parameter = $\dfrac{\langle j_2|L'|j_1\rangle}{\langle j_2|L|\ j_1\rangle}$

As has already been pointed out |51|, the 2^- ß 2^+ ɣ 0^+ cascade in Rb^{86} offers a comparatively large A_2-term. This indicates a considerable linear polarization of the γ-transition, which has to be considered in the circular polarization measurement according to equation (B 5).

For cylindrical Compton scattering arrangements, however, as used in the experiment reported in chapter II the $P_\ell(\theta,W,\psi)$-term of equation (B 6) averages out because all angles ψ are equally possible.

References

1. Wahlborn, S.: Nucl. Phys. 58, 209 (1964)
2. Robinson, R.L., Langer, L.M.: Phys. Rev. 112, 481 (1958)
3. Deutsch, J.P., Grenacs, L., Lehmann, J., Lipnik, P.: J. Phys. Rad. 22, 659 (1961)
4. Thompson, R.H., Casper, K.J.: Nucl. Phys. 72, 106 (1965)
5. Spejewski, E.H.: Nucl. Phys. 82, 481 (1966)
6. Daniel, H., Collin, W., Kuntze, M., Margulies, S., Martin, B., Mehling, O., Schmidlin, P., Schmitt, H.: Nucl. Phys. A118, 689 (1968)
7. Viano, J.B., Renard, J.C., Menet, J., de Saintignon, P., Laverne, A., Depommier, P.: J. de Physique 30, 763 (1969)
8. Fischbeck, H.J., Wilkinson, R.G.: Phys. Rev. 120, 1762 (1960)
9. Hamilton, J.H., Pettersson, B.-G., Hollander, J.M.: Arkiv Fysik 19, 249 (1961)
10. Alberghini, J.E., Steffen, R.M.: Phys. Lett. 7, 85 (1963)
11. Simms, P.C., Namenson, A., Wei, T.H., Wu, C.S.: Phys. Rev. 138, B777 (1965)
12. Rao, W.V.S., Rao, K.S., Sastry, D.L., Jnanananda, S.: Proc. Phys. Soc. 87, 917 (1966)
13. Hocquenghem, J.C., Berthier, J.: quoted in Ref. 7.
14. de Beer, A.: Thesis, Vrije Universiteit te Amsterdam (1968)
15. Lachkar, J.: Rapport CEA - R - 3659 (1969)
16. Boehm, F., Rogers, J.D.: Nucl. Phys. 45, 392 (1963)
17. Kneissl, U.: Z. Naturforsch. 20a, 1364 (1965)
18. Mehling,O., Daniel, H.: Nucl. Phys. A124, 320 (1969)
19. Bosken, J.J., Ohlms, D.E., Simms, P.C.: Phys. Rev. C3, 1168 (1971)
20. Holden, J.E., Kolata, J.J., Daehnick, W.W.: Phys. Rev. C6, 1305 (1972)
21. Montague, D.G., Ramavataram, K., Chant, N.S., Davies, W.G., Kitching, J.E., Latchie Mc., N., Morton, J.M.: Z. Physik 261, 155 (1973)
22. Braslau, N., Brink, G.O., Khan, J.M.: Phys. Rev. 123, 1801 (1961)
23. Ackermann, F., Platz, I., zu Putlitz, G.: Z. Physik 260, 87 (1973)
24. Simms, P.C.: Phys. Rev. 138, B784 (1965)

25. Kopytin, I.V., Batkin, I.S.: Sov. J. Nucl. Phys. 11, 192 (1970)
26. Manthuruthil, J.C., Poirier, C.P., Sastry, K.S.R., Petry, R.F., Cantrell, B.K., Wilkinson, R.G.: Phys. Rev. C4, 960 (1971)
27. Schweitzer, J.S., Simms, P.C.: Nucl. Phys. A198, 481 (1972)
28. Wischhusen, R.: Thesis, Universität Karlsruhe (1973)
29. Wischhusen R., Behrens, H.: Proc. Int. Conf. on Angular Correlations in Nuclear Disintegration, p. 315, Delft, 1970, ed. v. Krugten, H., v. Nooijen, B.
30. Schopper, H.: Weak Interactions and Nuclear Beta Decay (North Holland, Amsterdam, 1966)
31. Appel, H.: Numerical Tables for Angular Correlation Computations, Landolt Börnstein new Series I/3 (Springer, Berlin, 1968)
32. Behrens, H., Jaenecke, J.: Numerical Tables for Beta Decay and Electron Capture, Landolt-Börnstein new Series I/4 (Springer, Berlin, 1969)
33. Goudsmit, S., Saunderson, J.L.: Phys. Rev. 57, 24 (1940), Phys. Rev. 58, 36 (1940)
34. Frankel, S. : Phys. Rev. 83, 673 (1951)
35. Gupta, N.K., Sastry, S.R.: Proc. Int. Conf. on Angular Correlations in Nuclear Disintegration, p. 156, Delft, 1970, ed. v. Krugten, H., v. Nooijen, B.
36. Müller, H.-W.: Diplomarbeit, Universität Karlsruhe (1973)
37. Schopper, H.: Nucl. Instr. Meth. 3, 158 (1958)
38. Schopper, H., Behrens, H., Müller, H., Görres, J., Jüngst, W., Appel, H.: Nucl. Instr. Meth. 49, 277 (1967)
39. Bürk, K.: Thesis, Universität Karlsruhe (1974)
40. Talmi, I.: Nucl. Phys. A172, 1 (1971)
41. Shlomo, S., Talmi, I.: Nucl. Phys. A198, 81 (1972)
42. Kitching, J.E., Davies, W.G., Darcey, W.J., Mc Latchie, W., Morton, J.: Nucl. Phys. A177, 433 (1971)
43. Kitching, J.E.: Z. Phys. 258, 22 (1973)
44. Ogawa, K.: Phys. Lett. 45B, 214 (1973)
45. Arima, A., Hamamoto, I.: Ann. Rev. Nucl. Science 21, 55 (1971)
46. Alaga, G.: Nucl. Struct. and Nucl. Reactions Proc. of the Int. School of Phys. 'Enrico Fermi', Course IX ed. by Jean, M., Ricci, R.A., Academic, New York 1969
47. Behrens, H., Bühring, W.: Nucl. Phys. A162, 111 (1971)
48. Paul, H., Tatzber, W.: Acta Phys. Austriaca 25, 36 (1967)
49. Motz, J.W., Olsen H., Koch, H.W.: Revs. Mod. Phys. 36, 881 (1964)

50. Bonham, R.A., Strand, T.G.: J. Chem. Phys. 39, 2200 (1963)
51. Appel, H., Bürk, K., Behrens, H.: Proc. Int. Conf. on Angular Correlations in Nucl. Disintegration, p. 319, Delft, 1970, ed. v. Krugten, H., v. Nooijen, B.